Published in final edited form as:
J Comp Neurol. 2008 December 20; 511(6): 832–846. doi:10.1002/cne.21866.

Increased AMPA receptor GluR1 subunit incorporation in rat hippocampal CA1 synapses during benzodiazepine withdrawal

Paromita Das[a,ψ], **Scott M. Lilly**[a,b,ψ], **Ricardo Zerda**[d], **William T. Gunning III**, **Francisco J. Alvarez**[c,d,†], and **Elizabeth I. Tietz**[a,b,†]

[a] Department of Physiology and Pharmacology, University of Toledo College of Medicine, Health Science Campus, Toledo, OH 43614, USA

[b] Cellular and Molecular Neurobiology Program, University of Toledo College of Medicine, Health Science Campus, Toledo, OH 43614, USA

[c] Departments of Pathology and Biochemistry and Cancer Biology 3000 Arlington Avenue, University of Toledo College of Medicine, Health Science Campus, Toledo, OH 43614, USA

[d] Department of Neuroscience, Cell Biology and Physiology 3640 Colonel Glenn Highway, Wright State University, Dayton OH 45401, USA

Abstract

Prolonged benzodiazepine treatment leads to tolerance and increases the risk of dependence. Flurazepam (FZP) withdrawal is associated with increased anxiety correlated with increased AMPAR-mediated synaptic function and AMPAR binding in CA1 pyramidal neurons. Enhanced AMPAR synaptic strength is also associated with a shift toward inward rectification of synaptic currents and increased expression of GluR1, but not GluR2 subunits, suggesting augmented membrane incorporation of GluR1-containing, GluR2-lacking AMPARs. To test this hypothesis, the postsynaptic incorporation of GluR1 and GluR2 subunits in CA1 neurons after FZP withdrawal was examined using postembedding immunogold quantitative electron microscopy. The percentage of GluR1 positively-labeled stratum radiatum (SR) synapses was significantly increased in FZP-withdrawn rats (88.2 ± 2.2%) compared to controls (74.4 ± 1.9%). In addition, GluR1 immunogold density was significantly increased by 30% in SR synapses in CA1 neurons from FZP-withdrawn rats compared to control rats (FZP: 14.1 ± 0.3 gold particles/μm; CON: 10.8 ± 0.4 gold particles/μm). In contrast, GluR2 immunogold density was not significantly different between groups. Taken together with recent functional data from our laboratory, the current study suggests that the enhanced glutamatergic strength at CA1 neuron synapses during benzodiazepine withdrawal is mediated by increased incorporation of GluR1-containing AMPARs. Mechanisms underlying synaptic plasticity in this model of drug dependence are therefore fundamentally similar to those that operate during activity-dependent plasticity.

Keywords

Electron microscopy; LTP; Plasticity; Hippocampus; Dependence; Glutamate

Corresponding Author: Elizabeth I. Tietz, PhD, Department of Physiology and Pharmacology University of Toledo College of Medicine (Formerly Medical University of Ohio), Health Science Campus, 3000 Arlington Ave., Mailstop 1008, Toledo, OH 43614., Tel: (419)383-4170; Fax: (419)383-2871; E-mail: liz.tietz@utoledo.edu.
ψP.D. and S.M.L contributed equally to the work.
†An equal contribution was made from the laboratories of F.J.A. and E.I.T.
Associate Editor: Oswald Steward

Introduction

Fast excitatory neurotransmission in the mammalian central nervous system (CNS) is predominantly mediated by alpha-amino-3-hydroxy-5-methyl-4-isoxazolepropionic acid type glutamate receptors (AMPARs). Mature ionotropic AMPARs are expressed throughout the brain and are highly clustered at postsynaptic sites where they respond rapidly to synaptically released glutamate. AMPARs are tetramers composed of combinations of four subunits: GluR1-4 (Petralia and Wenthold, 1992; Wenthold et al., 1996). GluR1, GluR3 and GluR4 subunits form calcium-permeable inwardly-rectifying channels, while GluR2 subunits form calcium-impermeable channels with linear or outward rectification (Jonas and Burnashev, 1995; Washburn et al., 1997). Distinct populations of GluR1/2 and GluR2/3 containing hetero-oligomeric complexes are present in the mature hippocampus (Wenthold et al., 1996). Activity-dependent changes in synaptic strength such as long-term potentiation (LTP) are thought to be primarily due to trafficking and insertion of GluR1-containing AMPARs into excitatory synapses, which are subsequently replaced by a constitutively recycled pool of GluR2/3 receptors (Hayashi et al., 2000; Shi et al., 2001; Malinow and Malenka, 2002; Lee at al., 2003; Nicoll, 2003; Plant et al., 2006; Brown et al., 2007; Greger and Esteban, 2007; Elias and Nicoll, 2007).

Similar mechanisms underlying activity-dependent glutamatergic synaptic plasticity may also play important roles in neural and behavioral adaptations during development of dependence and addiction resulting from chronic exposure to drugs of abuse (Nestler, 2002; Kauer and Malenka, 2007). For example, chronic cocaine increases the insertion of GluR1-containing AMPARs in dopaminergic synapses in the ventral tegmental area (VTA) and nucleus accumbens of rodents (Carlezon et al., 1997; Boudreau et al., 2007). Enhanced glutamatergic strength is also involved in the development of dependence to alcohol or morphine (Molleman and Little, 1995; Sanchis-Segura et al., 2006). Chronic morphine treatment raises AMPAR GluR1 subunit levels in VTA and morphine-induced tolerance and dependence is reduced in mice deficient in AMPAR GluR1 subunits (Fitzgerald et al., 1996; Vekovischeva et al., 2001).

Benzodiazepines, including diazepam and flurazepam (FZP), are widely used sedative-hypnotics, anxiolytics, and anticonvulsants that exert their clinical effects by allosteric augmentation of GABA-gated chloride currents through central γ-amino butyric acid type-A receptors (GABAR) (Wafford, 2005). Despite their acute efficacy, long-term exposure to these drugs results in tolerance and dependence, which increase their potential for abuse and limit their clinical utility (Griffiths and Johnson, 2005). While development of tolerance has been primarily associated with GABAR dysfunction (Bateson, 2002; Wafford, 2005), it has been long known that anxiety, seizures and other signs of benzodiazepine dependence could be suppressed by glutamate antagonists (Steppuhn and Turski, 1993). The hippocampus plays an important role in the expression of anxiety and seizures and is an important site of acute benzodiazepine anxiolytic and anticonvulsant actions (Ashton et al., 1988; McNaughton and Gray, 2000; Engin and Treit, 2007). Moreover, recent evidence from our laboratory and others suggests that enhanced glutamatergic transmission in the hippocampus is associated with benzodiazepine withdrawal phenomena (Izzo et al., 2001; Van Sickle et al., 2004; Allison and Pratt, 2006; Xiang and Tietz, 2007).

LTP of hippocampal CA1 synapses is usually associated with learning (Whitlock et al., 2006), but similar changes in excitability within the neural circuits that subserve LTP might also have more undesirable effects. For example, a subset of CA1 neurons displaying strong LTP were shown to underlie hippocampal seizure susceptibility and initiate epileptiform activity (Chang et al., 2007). As noted above, LTP-like mechanisms have been related to synaptic plasticity in other brain regions after chronic drug use. Thus, LTP-like synaptic

plasticity in the CA1 region might contribute to increase hippocampal glutamate neurotransmission during development of benzodiazepine withdrawal-anxiety.

Previous studies showed that both AMPAR-mediated miniature excitatory postsynaptic currents (mEPSCs) and AMPAR binding were enhanced in hippocampal CA1 pyramidal neurons following one-week FZP administration, concomitant with the appearance of CA1 neuron hyperexcitability and anxiety-like behavior in FZP-withdrawn rats (Van Sickle et al., 2004). Moreover, anxiety-like behavior in this model was prevented by pretreatment with an AMPAR antagonist (Xiang and Tietz, 2007). Enhanced glutamatergic strength was also manifested by the increased amplitude of glutamate-evoked whole-cell currents recorded in acutely isolated hippocampal CA1 pyramidal neurons. The AMPAR currents also showed a shift towards inward rectification in both dissociated neurons and hippocampal slices, suggesting postsynaptic incorporation of AMPARs lacking the GluR2 subunit. The changes in AMPAR function during withdrawal from prolonged FZP exposure were associated with increased GluR1 expression detected using immunoblots and with immunofluorescence (Song et al., 2007). These findings provide strong evidence that enhanced AMPAR function in rat hippocampal CA1 neurons during benzodiazepine withdrawal share similarities with mechanisms underlying activity-dependent synaptic plasticity, such as LTP.

The goal of the present study was to investigate whether AMPAR GluR1 subunits are specifically incorporated into hippocampal CA1 synapses during benzodiazepine withdrawal in an LTP-like fashion. Electron microscopy postembedding immunogold labeling demonstrated increased density of GluR1 subunits at synapses during benzodiazepine withdrawal without significant changes in GluR2 subunit synaptic content. These findings provide further evidence that adaptations associated with dependence on drugs of abuse are similar to mechanisms underlying activity-dependent synaptic plasticity.

Materials and Methods

Chronic Benzodiazepine Treatment

Experimental protocols involving the use of vertebrate animals were approved by the University of Toledo College of Medicine (formerly the Medical University of Ohio), Institutional Animal Care and Use Committee (IACUC) and conformed to the National Institutes of Health guidelines. All efforts were made to minimize animal distress.

After a 2–3 day acclimation period during which 0.02% saccharin water was available, juvenile male Sprague-Dawley rats (Harlan, Indianapolis, IN) were offered FZP in 0.02% saccharin water as the sole source of drinking water for 1 week. The target for the FZP group was an average dose of 100 mg/kg/day for the first three days, and 150 mg/kg/day for the following four days. Animals that did not achieve a weekly average of 120 mg/kg/day were excluded. After drug removal, animals were given saccharin water for an additional 2 days prior to euthanasia, and tissue preparation for analysis. At the time of euthanasia the animals were between 35 to 40 postnatal days of age. Controls received only saccharin water in parallel to the experimental group during acclimation, 1-week treatment, and withdrawal period.

The concentration of FZP (100–150 mg/kg) offered to rats was appropriate to its relative potency and oral bioavailability (Chouinard, 2004). One-week FZP treatment results in a brain concentration of FZP and its active metabolites of 1.2 μM, equivalent to 0.6 μM diazepam (Xie and Tietz, 1992). Due to the short half-life of FZP in rat brain (<12 hr), the level of FZP and its active metabolites is negligible in the hippocampus 2 days after FZP withdrawal (Xie and Tietz, 1992; Van Sickle et al., 2004). This dosing regimen has been shown to reliably induce manifestations of both benzodiazepine tolerance and dependence

(Tietz et al., 1999; Van Sickle et al., 2004). Rats treated in this way show a progressive increase in AMPA mEPSC amplitude from day 1 (~15–30%) to day 2 (~30–50%) after benzodiazepine withdrawal. Both the increase in AMPAR function and the associated anxiety-like behavior are transitory and return to control levels within 4 days after treatment cessation (Van Sickle et al., 2004). Seizure activity is not observed at any time during withdrawal from 1-week FZP treatment.

Transcardial Perfusion and Tissue Preparation

For electron microscopic studies, rats were anesthetized with an intraperitoneal injection of pentobarbital (100 mg/kg). A vascular rinse solution (pH 7.4) containing (mM) 136 NaCl; 3.5 KCl; 6 mM $NaHCO_3$ was bubbled with 95% O_2/5% CO_2 for 15 min. After bubbling and prior to perfusion, heparin (5 units/ml) was added to the vascular rinse. Rats were rapidly perfused via the aorta with 50 ml of the equilibrated vascular rinse solution, followed by perfusion with 300–350 ml fixative containing 4% paraformaldehyde and 0.5% glutaraldehyde in 0.1 M phosphate buffer (PB), pH 7.4. Blocks containing bilateral hippocampii were hemisected and postfixed in the same solution for 4 hr.

Freeze slamming, cryosubstitution and low temperature embedding

Coronal vibratome sections (500 μm) were exposed to 1% sodium borohydride in PB for 60 min, rinsed 6 × 30 min, placed in 4% glucose overnight (4°C), equilibrated in glycerol (10, 20, and 30% in 0.01 M PBS, pH 7.4), then slammed to a pre-cooled copper mirror (−190°C, Leica EM CPC, Bannockburn, IL). For cryosubstitution and low temperature embedding, tissues were transferred to Leica EM AFS and treated as follows: 12 hr in 1% uranyl acetate in methanol (−80° C), 4 × 30 min in absolute methanol (this and following at −50° C), 2 hr each in 50%, 75%, 100% lowicryl HM20, and 2 × 8 hr in 100% lowicryl. Sections were then flat-embedded using lowicryl in between glass coverslips coated with formen-trenmittel (Electron Microscopy Sciences, Ft. Washington, PA), and polymerized with UV light (48 hr at −50° C, 72 hr at 0° C, 48 hr at +20° C). The CA1 area of the hippocampus was excised and glued to EM blocks. Ultrathin sections were obtained (65–70 nm thickness; silver/gold sections) and collected on formvar-coated 200-mesh nickel grids.

Antibody characteristics

Anti-GluR1—A rabbit anti-GluR1 subunit antibody, kindly donated by Dr. R. Wenthold, NIDCD, Bethesda, MD, USA was used in initial studies. The Wenthold antibody was obtained from host rabbit by injecting a BSA-conjugated synthetic peptide, (SHSSGMPLGATGL) corresponding to amino acid residues 877–889 of the carboxy terminus (C-terminus) of the rat GluR1 subunit. Using this antibody, immunoblots of GluR1 transfected cells and solubilized rat brain membranes showed a single band corresponding to a molecular weight of ~108 kDa (Wenthold et al., 1992). The Wenthold rabbit polyclonal anti-GluR1 antibody has been further characterized using light and electron microscopy (Petralia and Wenthold, 1992). Further studies were performed using a commercially available rabbit polyclonal anti-GluR1 antibody (Chemicon International, Temecula, CA; Cat# AB1504, Lot# 0508008855). The Chemicon anti-GluR1 antibody was obtained by injecting the same C-terminus peptide of rat GluR1 (SHSSGMPLGATGL) conjugated to KLH into host rabbit (manufacturer's technical information). This antibody has been extensively characterized by immunoblot and light and electron microscopic techniques and used in several publications reporting the distributions of glutamate receptors in diverse regions of the mammalian brain (Joshi et al., 2004; King et al., 2006; Kim et al., 2006). Immunoblot analysis of this antibody in the rat brain showed a single band of ~110 kDa, co-migrating with GluR1 subunit expressed in transfected cells (manufacturer's technical

information). In addition, the specificity of this antibody in CA1 synapses has been tested in GluR1 knockout mice using immunocytochemical techniques (Zamanillo et al., 1999).

Anti-GluR2—The Chemicon anti-GluR2 antibody used in this study (rabbit polyclonal anti-GluR2 antibody, Chemicon International, Temecula, CA; Cat# AB1768, Lot# 0702052022) was obtained by injecting the host rabbit with a synthetic immunogenic peptide (VAKNPQNINPSSSQNS) corresponding to amino acid residues 827–842 of rat GluR2 C-terminus conjugated to BSA. Immunoblot analysis of rat brain showed a single band of ~108 kDa and immunocytochemical analysis of transfected cells showed no cross-reactivity with GluR1, GluR3 or GluR4 subunits (Petralia et al., 1997). The specificity of this antibody was further tested in tissue from a GluR2 knockout (KO) mouse. Ultrathin sections from the hippocampal region from a KO and a matching wild-type (WT) littermate were kindly donated by Drs. Ronald Petralia and Ya-Xian Wang (Sans et al., 2003). Sections from KO and WT were immunolabeled in parallel using identical conditions to those described below. In addition, some WT sections were processed omitting the primary antibody. Immunolabeling of synapses in the GluR2 KO was negligible, with only a few synapses labeled in the KO, usually with only one gold particle. Similar labeling was observed in WT tissue after omitting the primary antibody (see Results), suggesting that the labeling originated from a low-level of non-specific absorption of secondary antibodies and was clearly different in density and incidence to the specific PSD labeling analyzed.

Post-embedding immunogold labeling

Grids were wet in Tris-buffered saline with 0.1% Triton X-100 (TBST) pH 7.6, and then incubated for 30 min in 1:10 normal goat serum (Cat# 9023, Sigma-Aldrich, St. Louis, MO) containing 0.1 % Na-borohydride and 50 mM glycine. In initial experiments, grids were etched for 3 sec in sodium ethanolate. A saturating concentration of NaOH was dissolved in 70% ethanol at least 24 hr before use. The solution was used for several days until its transparency was lost. Sections were then washed in TBST and incubated for 2 hr at room temperature in rabbit anti-GluR1 subunit antibody (1:50, R. Wenthold). Although etching increased immunolabeling, it also clearly affected ultrastructural definition and contrast. Using a more concentrated solution (1:10) of the commercial rabbit polyclonal anti-GluR1 subunit antibody, the labeling efficiency at CA1 asymmetrical synapses was increased even without etching, therefore this step was omitted. Separate grids were also incubated without etching in a rabbit polyclonal anti-GluR2 subunit antibody (1:50, Chemicon). After 2 hr incubation in the respective primary antibodies at room temperature, grids were transferred to 4°C for overnight incubation. Grids were rinsed 3 × 5 min in TBST (pH 7.6), then TBST (pH 8.2) and incubated 2 hr in goat anti-rabbit IgG conjugated to 10 nm gold particles (EMGAR10, BBI, United Kingdom) diluted 1:25 in TBST (pH 8.2). After rinsing 3 × 5 min in TBST (pH 8.2) and filtered (0.22 μm) distilled water (dH_20), grids were contrasted with 5% uranyl acetate in filtered dH_20 and lead citrate, 5 and 4 min, respectively.

Data Analysis

Electron Microscopy

Reacted ultrathin sections were analyzed in a Philips 201 EM electron microscope at 70 kV and the PSDs in the stratum oriens and radiatum (SO and SR) of CA1 imaged. Given that pyramidal cells outnumber interneurons in the CA1 region of the hippocampus by approximately 20:1, and contain far more excitatory synapses per cell (Megias et al., 2001), the presumed contribution of excitatory synapses from interneurons was considered negligible in this analysis. The analysis was performed in single cross-sections of synapses rather than in synapses reconstructed through serial sections. This allowed the analysis of

relatively larger samples of synapses per rat (~30 to 70 synapses per animal sampled in 1–3 different blocks).

Areas within approximately 100 μm of the stratum pyramidale (SP) border in SO and SR of the CA1 region of the hippocampus were scanned, and digital images of asymmetric junctions representing excitatory synapses (Megias et al., 2001) were acquired at a magnification of X 36,000 (Gatan BioScan Camera) by an observer blind to the experimental groups. An image was acquired for every asymmetric synapse encountered, unlabeled or immunogold labeled, in random surveys of the target region. All synapses demonstrating a clear synaptic cleft were included in the sample. Thus, synapses included in the analyses were all cut in a similar plane approximately perpendicular to the synapse, which avoids problems associated with differences in immunogold access, profile size and identification of obliquely or tangentially cut PSDs. In initial studies the GluR1 antibody provided by R. Wenthold was used. Approximately 50 images were obtained from immunoreacted sections (1:50 dilution) derived from matched pairs of control and FZP-withdrawn rats (n=3 per group) and analyzed with Image Pro-Plus software (v. 5.0 Media Cybernetics). Some images had more than one synapse, thus the number of synapses analyzed varied from 48 to 79 in different animals within a region. In this first experimental series, changes in GluR1 immunoreactivity between the SR and SO regions were compared. Subsequently, GluR1 and GluR2 immunoreactivity were compared specifically in the SR region, which showed the largest changes in GluR1, as expected. For this second experimental series, 30 to 70 images were obtained from matched pairs of a different set of control and experimental animals. Five control and 5 FZP-withdrawn rats were analyzed using the commercially available anti-GluR1 antibody (Chemicon, dilution 1:10). For the study with the anti-GluR2 antibody (Chemicon, dilution 1:50) tissues from the same set of animals (control, n=4 rats; FZP-withdrawn n=3 rats) were compared. In these experiments, a larger proportion of synapses in control animals were labeled using Chemicon's anti-GluR1 antibody, diluted 1:10 than Wenthold's anti-GluR1 antibody diluted 1:50. Despite different sensitivities in detecting synaptic GluR1, an increase in immunolabeling was found in the SR region of FZP-withdrawn animals compared to their matched controls using both anti-GluR1 antibodies in the two different experimental series.

The numbers of gold particles inside the PSD, or at a maximum 20 nm from the surrounding edge of the PSD (see Figure 1A–C) including those falling in the synaptic cleft, were counted in all synapses sampled and defined as postsynaptic labeling. Gold particles that were outside the 20 nm surrounding edge of the PSD and fell on the presynaptic membrane were not counted. Labeling precision with 10 nm colloidal gold conjugates of complete IgGs, using indirect immunolabeling methods has been estimated to be within 20–30 nm of the epitopes (see Hainfeld 1987 and Herman et al., 1996; Matsubara et al., 1996). Immunogold densities were estimated as particles per linear μm of PSD. Perisynaptic labeling was defined as immunogold labeling within 100 nm lateral to either side of the PSD along the plasma membrane, excluding the 20 nm edge zone were colloidal gold particles were considered associated with the PSD itself (Fig. 1A–C). 10

Statistical Analyses

The number of synapses labeled in FZP-withdrawn neurons was compared by Mann-Whitney U test to the expected value obtained from control hippocampii, and expressed as a percent of labeled synapses for comparison between groups, which contained different numbers of synapses in each sample. Density of labeling was estimated as the number of gold particles divided by PSD length in microns and compared by Student's *t*-test between FZP-withdrawn and control groups. Measures of PSD size were compared between groups using ANOVA with post-hoc analysis by Bonferroni's multiple comparison test. A regression analysis was used to evaluate the relationship between the number of GluR1- or

GluR2-immunogold particles and PSD length within the aggregate of synapses from each control and experimental animal. The differences in lengths between control and FZP-withdrawn immunonegative and immunopositive PSDs were compared for both GluR1- and GluR2-labeled synapses by one-way ANOVA with post-hoc analysis by Bonferroni's multiple comparison test. The relative frequency distribution of different numbers of GluR1- or GluR2-immunogold gold particles in synapses of FZP-withdrawn versus control neurons was compared by χ^2 analysis. Comparison of numbers of particles (0 to ≥9) between groups was by Mann-Whitney U test. All data are reported as mean ± SEM. The significance level was set at $p < 0.05$.

To more precisely determine the distribution of gold particles within synapses, the position of gold particles was measured relative to the postsynaptic membrane in a representative subset of GluR1- and GluR2-labeled synapses in control and experimental groups. The distance between the center of each gold particle and the outer leaflet of the postsynaptic membrane was measured with Image Pro-Plus software (v. 5.0 Media Cybernetics), grouped into 4 nm bins and plotted against the number of gold particles.

EM micrographs in Figures 1, 2 and 4 were composed in Photoshop 5.0 (Adobe Systems, San Jose, CA or CorelDraw 12, Fremont, CA) from digitized images with minor adjustments to brightness and contrast. Camera scratches and dust particles in Figure 1 (presented as full field of view) were digitally removed. Data were statistically analyzed and Figures 3 through 8 generated using Prism™ 4.0 software (GraphPad Software Inc, San Diego, CA).

Results

To determine possible changes in the number of GluR1 and GluR2 AMPA receptor subunits during FZP withdrawal, immunoreactivity for these subunits was examined in synapses on the dendritic regions of CA1 hippocampal neurons. These hippocampal regions show the highest changes in dendritic AMPAR binding during FZP withdrawal (Van Sickle and Tietz, 2002). Moreover, diazepam withdrawal anxiety was also associated with a significant enhancement of immunolabeling in hippocampal CA1 pyramidal neuron dendritic fields (Izzo et al., 2001).

Specificity of immunolabeling, regions of analysis, definition of immunolabeled synapses

GluR1- and GluR2-immunoreactivity was highly localized to synaptic sites with little immunoreactivity in the extrasynaptic membrane or on the neuropil (Fig. 1A,B). Synaptic labeling was analyzed in the PSD and surrounding 20 nm region (see Materials and Methods) while perisynaptic labeling was quantified in the plasma membrane within a 100 nm distance from the PSD (excluding the 20 nm juxta-PSD region) (Fig. 1B,C). GluR1 antibodies included one donated by R. Wenthold (diluted 1:50) and one commercial (diluted 1:10; Chemicon). The GluR2 antibody used was commercial (diluted 1:50; Chemicon).

The level of non-specific labeling was determined by placing twenty-five test rectangles of average length and width (0.22 μm and 0.045 μm, respectively) on each image (see Fig. 1D). The size of the test rectangles was empirically determined to match the average PSD size determined in our initial studies. The probabilities of one, two, three or more particles falling on top of a region of size similar to a PSD by random chance was then calculated for each image and averaged to provide an estimate for each immunoreaction and animal (Fig. 1E). Only gold particles whose center was within the rectangle were counted. Gold particles within rectangles that randomly fell on PSDs were included. Test rectangles that fell on top of regions with only resin (no tissue), areas that were obvious artifacts (holes in lowicryl, precipates) or the lumen of capillaries were not included in the analyses. In the 45 to 55

images used in GluR1 analyses for each control or FZP-withdrawn animal 1231±60 and 1277±38 test rectangles were analyzed, respectively. Fewer images were analyzed for the GluR2 antibody, but nevertheless these included analysis of 775±59 and 763±48 test rectangles in control and FZP-withdrawn animals. A similar analysis was performed in images obtained from WT and GluR2 KO mice tissue sections immunolabeled with the GluR2 antibody or omitting the primary antibody (2108, 2179 and 918 rectangles in 87, 90 and 38 images, respectively). The same secondary antibodies were used for GluR1 and GluR2 immunolabeling.

The probability of finding one or more particles in test rectangles was less than 3% in either SR or SO using the Wenthold anti-GluR1 antibody, diluted 1:50 and less than 5% using the commercial anti-GluR1 and anti-GluR2 antibodies diluted 1:10 and 1:50, respectively (Fig. 1E, only SR was tested). In sections from WT mice immunolabeled with GluR2 antibodies the probability of finding ≥ 1 particle was 1% and dropped to 0.4% in KO sections, suggesting that some of this immunolabeling might represent specific labeling of non-synaptic pools of GluR2 subunits. After omitting the primary antibody in WT tissue the probability of labeling in test rectangles was similar to that in KO tissue (0.3%), suggesting that the true level of background staining in the neuropil is less than half of the low levels estimated with test rectangles.

It is possible however, that PSDs are sites of preferential antibody absorption and contain levels of non-specific labeling higher than observed in test rectangles placed randomly in the neuropil. To estimate the extent of non-specific PSD labeling the number of immunolabeled PSDs was determined in sections from GluR2 KO and WT mice, after omitting the primary antibody. In both cases the percentage of synapses containing at least one gold particle was similar (9% in KO tissue, n=100 synapses sampled, and 8% in WT tissue after omitting the primary antibody, n=50 synapses sampled), and less than WT synapses immunolabeled with GluR2 antibodies (35%, n=100 synapses). These results confirm the specificity of the commercial GluR2 antibody used. The specificity of the commercial GluR1 antibody has previously been confirmed in GluR1 KO tissue (Zamanillo et al., 1999). In addition, the data indicate that the error of considering one gold particle as positive labeling is small and always less than 10%. Therefore, synapses containing just one gold particle were defined as immunopositive.

AMPAR GluR1 subunit immunoreactivity is increased in hippocampal CA1 synapses during FZP-withdrawal

Preliminary analyses compared the proximal regions of basal and apical dendrites located in SO and SR, respectively, using the GluR1 antibody donated by R. Wenthold (diluted 1:50). There was a significant increase in the number of particles per synapse in both the SO (CON: 0.59±0.01; FZP: 0.77±0.03, p=0.01, Student's t-test) and SR regions (CON: 0.51±0.05; FZP: 0.83±0.03, p <0.01). However, the percentage of unlabeled synapses in controls was very high (~60–65% in SO and SR regions) in these immunolabeled preparations. Many of these non-immunoreactive synapses likely represent false negatives and therefore hampered accurate estimation of changes in the number of labeled synapses between control and experimental tissues.

To expand on these findings, additional studies were focused in the SR region in additional matched pairs of control and FZP-withdrawn rats (n=5 rats/group). In the latter studies a commercial GluR1 polyclonal antibody was used at a lower dilution (1:10, Chemicon). In these preparations there was a higher degree of labeling, without a significant increase in non-specific labeling and the percentage of unlabeled synapses was <30%. Figure 2 illustrates representative examples of synapses labeled with the anti-GluR1 antibody (Chemicon) in control (A, B, and C) and FZP-withdrawn rats (D, E, and H). The percentage

of synapses demonstrating GluR1 AMPAR immunogold labeling (Fig. 3A) was significantly increased in the SR region in FZP-withdrawn rats (88.2±2.2%, n=5 rats, 51 to 59 synapses per animal) compared to controls (74.4± 1.9%, n=5 rats, 46 to 67 synapses per animal, p=0.002, Student's t-test). In the collection of immunolabeled synapses (i.e., containing at least one gold particle), immunogold density was also significantly higher in FZP-withdrawn rats (14.1±0.3 particles/μm, n=5 rats) compared to controls (10.8±0.4 particles/μm, n=5 rats, p<0.001) (Fig. 3B). Thus, both the percentage of labeled synapses (18.5% change) and GluR1 immunogold labeling density (30.5% change) increased significantly in the CA1 SR region of the hippocampus in FZP-withdrawn rats compared to controls.

PSDs in excitatory synapses of rat hippocampal CA1 SR region increase in size in response to FZP withdrawal

Long lasting changes in synaptic strength during activity-dependent forms of plasticity may require structural modifications such as increases in size, morphology and number of synapses (Harris et al., 2003; Lang et al., 2004). To determine if gross morphological changes occur during FZP withdrawal we measured the length, thickness and area of the PSD of CA1 excitatory synapses in the SR region of the hippocampus. The average PSD length (±SEM) from all control synapses (immunopositive and immunonegative) reacted with the anti-GluR1 antibody (Chemicon) was 0.239±0.009 μm (n=5 rats, PSDs sampled=263) compared to immunopositive and immunonegative synapses from FZP-withdrawn rats (0.270±0.008 μm, n=5 rats, PSDs sampled=277, F=476.8, df=5, p=0.001) indicating a significant elongation of the synapse. PSD thickness and total PSD cross-sectional area were not significantly different between FZP-withdrawn and control animals (see Table 1), but there was nevertheless a tendency for PSD cross-sectional areas to be larger in FZP-withdrawn animals. Average PSD areas were 0.014±0.001 μm^2 in control synapses compared to 0.017±0.001 μm^2 in experimental groups (n=5 rats/group, p=0.051, Student's t-test; n = 52.6±3.9 synapses analyzed per animal in control and 55.4±3.9 in FZP-withdrawn rats). The findings overall suggest that the PSD in excitatory synapses in the SR of the CA1 region of the hippocampus increased modestly in size in association with the incorporation of GluR1-containing AMPARs during FZP-withdrawal.

GluR2 subunits do not significantly increase in hippocampal CA1 synapses during FZP-withdrawal

Sections obtained from the same rats were used for GluR2 immunogold labeling (CON: n=4, FZP: n=3). Positively-labeled synapses were also identified as those with PSDs associated with one or more gold particles, as explained above. Figures 1 and 4 illustrate representative examples of synapses labeled with the anti-GluR2 polyclonal antibody (1:50, Chemicon) in control (Figs. 1 and 4A, B, and C) and FZP-withdrawn rats (Fig. 4D, E, and H). As with GluR1 antibodies, GluR2 immunogold labeling was present throughout the length of the PSD.

In contrast to GluR1, the percentage of synapses with GluR2 AMPAR labeling was not significantly different between the control (76.7±2.8%) and FZP-withdrawn (82.3±6.5%) groups (Fig. 5A). In contrast to GluR1-immunogold labeling, GluR2-immunogold density did not increase in the FZP-withdrawn groups (8.7±1.2 particles/μm) compared to controls (10.5±1.3 particles/μm) (Fig. 5B). The data however, showed a small trend towards an increase in the number of GluR2-immunolabeled synapses between control and FZP-withdrawn rats that might have attained statistical significance with a larger sample size. The percentage of synapses labeled in the control groups with either anti-GluR1 or GluR2 antibodies were similar (74.4±1.9% and 76.7±2.8% respectively). These proportions are similar to those reported previously in normal rat hippocampus (Petralia et al., 1999).

Unexpectedly, there were also no significant differences in the size of GluR2-labeled synapses (see Table 2) suggesting that the samples of GluR2- and GluR1-labeled synapses might somehow be different. Given that both subunits were found in a large proportion of synapses, the differences could arise if a subpopulation of larger PSDs containing only GluR1 subunits and/or a subpopulation of smaller PSDs containing only GluR2 subunits, each responded differently during FZP-withdrawal. Dual-labeling experiments will be necessary to analyze synapses with different proportions of each of these subunits. However, the GluR1 and GluR2 antibodies used in this study were developed in rabbit and our attempts to obtain dual labeling using two different methods to avoid cross-talk between primary antibody labeling, produced inconsistent results. Similarly, reliable labeling using a mouse monoclonal GluR2 antibody was not obtained.

Relationship between PSD size and GluR1- or GluR2-immunogold labeling

Studies using serial section analyses have demonstrated that PSD size is positively correlated with the number of AMPAR (GluR1, GluR2/3 and GluR4) immunogold particles (Nusser et al., 1998; Takumi et al., 1999). In our samples, scatter plots of immunogold particle numbers plotted as a function of PSD length in GluR1- and GluR2-immunolabeled synaptic profiles analyzed in single cross-sections, showed no significant correlation between PSD length and immunogold content (data not shown). However, these scatter plot analyses suggested possible differences in the size of AMPAR immunonegative PSDs compared to either GluR1- or GluR2-immunopositive PSDs. Namely, the average length of immunonegative PSDs in tissues reacted with the GluR1 antibody was not significantly different between control (0.208±0.005 μm) and FZP-withdrawn tissues (0.230±0.005 μm) (Fig. 6A). However, GluR1-immunopositive PSDs were significantly larger than their immunonegative counterparts and longer in the FZP-withdrawn group compared to control (CON: 0.250±0.010 μm; FZP: 0.274±0.010 μm, $p<0.01$). Similarly, in sections reacted with the GluR2 antibody, the lengths of immunonegative PSDs in control and FZP-withdrawn animals were not significantly different (CON: 0.214±0.001 μm; FZP: 0.199±0.002 μm) while immunopositive PSDs were significantly larger but did not show differences between control and FZP-withdrawn groups (CON: 0.272±0.007 μm; FZP: 0.270±0.020 μm, Fig. 6B). The present data obtained from large samples of synaptic profiles analyzed in single cross-sections are therefore consistent with previous serial section analyses showing that AMPAR immunonegative synapses are smaller in size than immunopositive synapses. Smaller immunonegative synapses have previously been interpreted as putatively “silent” with negligible or low AMPAR content (Takumi et al., 1999).

Perisynaptic labeling of AMPAR GluR1 and GluR2 subunits in hippocampal CA1 synapses during FZP-withdrawal

Perisynaptic labeling with the GluR1 antibody, defined as labeling 100 nm lateral to the PSD (see Fig. 1) was also observed and represented 10.7% and 6.9% of total GluR1 gold particles sampled at sites defined as postsynaptic labeling in control and FZP-withdrawn rats, respectively. Perisynaptic labeling in synapses labeled with the GluR2 antibody represented 2.4% and 3.9% of GluR2 gold particles sampled at postsynaptic sites from control and FZP-withdrawn tissues, respectively. GluR1 perisynaptic labeling was always low and if anything decreased in FZP-withdrawn animals.

Frequency distributions of GluR1- and GluR2-subunit labeling

To determine if some synapses express especially high or low levels of GluR1- or GluR2-containing receptors, the frequency distribution of immunogold particles in GluR1- and GluR2-labeled synapses was analyzed. A significant overall increase in the numbers of gold particles was observed in synapses from FZP-withdrawn rats compared to controls ($\chi^2=59.4$, df=9, $p=0.000$). In sections analyzed for GluR1 particles, relatively fewer numbers of

synapses from FZP-withdrawn rats lacked immunoreactivity compared to control synapses (Fig. 7A). Thus, the observed fraction of immunonegative synapses, lacking GluR1 particles was reduced ~2-fold in FZP-withdrawn rats (0.12±0.02) compared to controls (0.26±0.02, p=0.008, Mann-Whitney U test). The fraction of synapses expressing 7 and 8 gold particles in FZP-withdrawn rats was significantly increased when compared to controls (p=0.008). In sections analyzed for GluR2 particles, an overall change in distribution of gold particles across synapses between controls and FZP-withdrawn rats was observed (χ^2=77.8, df=9, p=0.000), however the observed fraction of synapses lacking GluR2 particles (0 particles) was not significantly different between groups (CON: 0.24 ± 0.03 and FZP: 0.18 ± 0.07; p=0.86, Mann-Whitney U test, Fig. 7B). There were also no significant differences in the fraction of labeled synapses with a given number of gold particles (1 to ≥9) between control and FZP-withdrawn groups (p>0.05, Mann-Whitney U test).

GluR1 and GluR2 AMPAR subunit immunogold labeling show similar distributions in PSDs of synapses from control and FZP-withdrawn rats

Quantitative analysis of GluR1 and GluR2 immunogold particle location in PSDs was performed to more precisely determine the distribution of synaptic labeling in relation to the postsynaptic membrane for each subunit and whether the distribution changed during FZP withdrawal. Labeling for both receptor subunits was highly localized within the PSD of the synapse. GluR1 immunolabeling distribution was analyzed in 67 synapses from a control and 56 synapses from an FZP-withdrawn rat, each representative of its group. Positions from the center of each gold particle to the outer leaflet of the postsynaptic membrane were measured with a resolution of ±2 nm (the pixel size in the X 36,000 and 1,024 × 1,024 digital images) and binned in 4 nm increments (0=outer edge of postsynaptic membrane, positive values represent the intracellular side, negative values the synaptic cleft side). As illustrated in Figure 8A, in control synapses most GluR1-immunogold particles (81.3%) were located on the postsynaptic side (i.e. positional value ≥0 in Fig. 9) and 52.9% within the first 25 nm (i.e. approximately half of the average width of the PSD) with a peak density +6 nm from the outer edge of the plasma membrane. This was similar in FZP-withdrawn animals.

Data for GluR2-labeling was obtained from 44 synapses from a representative control rat and 40 synapses from an FZP-withdrawn rat. The spatial distribution of GluR2-immunolabeling was also similar to GluR1 (peak +6 nm, 76.6% located on the postsynaptic side, 70.8% in first 25 nm), and was not different in FZP-withdrawn animals (Fig. 8B). In conclusion, both GluR1 and GluR2 immunoreactivity analyzed in the PSD were strongly associated with the postsynaptic membrane in both control and FZP-withdrawn animals.

Discussion

The present data provide ultrastructural evidence of a significant increase in AMPAR GluR1-mediated glutamatergic neurotransmission in excitatory synapses on the apical dendrites (SR) of hippocampal CA1 neurons during benzodiazepine withdrawal. The electron microscopy data agree with our and others' previous biochemical and functional studies demonstrating enhanced AMPAR-mediated mEPSC amplitude, AMPAR radioligand binding and GluR1 subunit expression at the light microscopic level (Izzo et al., 2001; Van Sickle and Tietz, 2002; Van Sickle et al., 2004), a shift toward inward rectification of synaptic AMPAR currents (Song et al., 2007) and an increase in GluR1, but not GluR2 subunit protein expression (Song et al., 2007), all of which are indicative of postsynaptic incorporation of GluR1-containing, but GluR2-lacking AMPARs and coincide with anxiety, a manifestation of withdrawal from chronic benzodiazepine treatment (Van Sickle et al., 2004; Xiang and Tietz, 2007).

Neurophysiological changes occurring during prolonged exposure to drugs of abuse have often been compared to those occurring in activity-dependent forms of plasticity such as LTP (Kauer and Malenka, 2007). A widely studied example of synaptic plasticity is the stimulus-induced potentiation of the Shaffer collateral-CA1 neuron glutamatergic pathway (Malenka and Bear, 2004). Numerous studies suggest an important role for enhanced expression of GluR1-containing AMPARs in LTP (Zamanillo et al., 1999, Jia et al., 1996), albeit transient (Plant et al, 2006; Hayashi et al., 2000). [However, see Adesnik and Nicoll, 2007 and Jensen et al., 2003]. Upon LTP induction there is a decrease in the number of synaptic failures, indicating a conversion of “silent” synapses (not containing AMPAR) to “non-silent” synapses, thought to depend on enhanced synaptic expression of GluR1-containing AMPARs (Malinow and Malenka, 2002; Poncer, 2003). This enhancement is accompanied by an increase in synapse size as Shaffer-collateral AMPAR-immunopositive synapses are larger, relative to putatively silent, AMPAR-immunonegative synapses (Takumi et al., 1999; Nusser et al., 1998).

The major findings of this study using post-embedding immunogold were a significant increase in the density of synaptic GluR1 immunolabeling (expressed as particles per μm), a significant increase in percentage of synaptic profiles immunopositive for GluR1 and a small increase in the length of GluR1 immunopositive PSDs in FZP-withdrawn rats. Synaptic incorporation of the GluR2 subunit remained unchanged. Enhanced incorporation of GluR1 subunits occurred in synapses of both apical and basal dendrites of CA1 neurons but a greater change was observed in GluR1 immunolabeling in SR (63% increase in labeling density) compared to SO (37% increase).

Labeling for both GluR1 and GluR2 subunits was predominant in the PSD and largely concentrated within 20 nm of the postsynaptic plasma membrane with a clear peak 6 nm intracellular from the outer surface of the plasma membrane. This localization is consistent with previous reports suggesting a postsynaptic membrane localization of AMPAR subunits. This localization also agrees with the C-terminal location of AMPAR GluR1 and GluR2 subunits on the cytoplasmic aspect of the postsynaptic plasma membrane at a distance from the membrane that coincides with the location of C-terminal-interacting PSD proteins and the C-terminus of the N-methyl-D-aspartate receptor (Khazaria and Weinberg, 1999; Sassoe-Pognetto and Ottersen, 2000, Valtschanoff et al., 2000). The width of labeling distributions obtained for each subunit are also consistent with the resolution of colloidal gold antibody probes, expected to locate epitopes within a 20–30 nm radius (Hainfeld 1987; Herman et al., 1996; Matsubara et al., 1996). Interestingly, GluR1 immunolabeling occupied a larger intracellular extension in the PSD than GluR2 immunolabeling. A plausible explanation for this difference is that GluR2 C-terminal epitopes are located closer to the plasma membrane than GluR1 C-terminal epitopes. Indeed, the C-terminus of GluR2 spans only 50 amino acids (a.a. 813–862) from the membrane and the peptide targeted by our antibodies occupies a mid-region (a.a. 827–842) (Petralia et al., 1997), compared to the more distal GluR1 C-terminal epitope targeted. The GluR1 C-terminus includes 81 amino acids (a.a. 809–889) and the peptide sequence recognized by the antibody is located at the very end of the tail (a.a. 877–889) (Wenthold et al., 1992). In any case, the labeling distributions obtained in both experimental groups are identical for each probe, indicating that the changes observed in FZP-withdrawn animals reflect increased occupancy of the postsynaptic membrane by GluR1 subunits.

The above-described changes at excitatory glutamatergic synapses occurring during benzodiazepine withdrawal were notably similar to those observed after LTP induction. However, in contrast to transient insertion of GluR2-lacking AMPAR observed in some forms of LTP, which are then gradually replaced by GluR2-containing AMPARs (Plant et al., 2006), our studies coupled with previous electrophysiological reports suggest that

prolonged administration of FZP and withdrawal induces a longer-lasting (at least 48 hr) change in AMPAR subunit composition, reflecting in all likelihood preferential synaptic incorporation of GluR1 subunit-containing receptors (Izzo et al., 2001; Song et al, 2007).

One proposed model of benzodiazepine dependence suggests that excitatory components are upregulated in an effort to maintain homeostasis in the face of benzodiazepine-mediated enhancement of GABAergic inhibition. In this scenario increased excitatory tone persists upon abrupt withdrawal of the benzodiazepines, and contributes to the expression of a withdrawal syndrome that includes anxiety (Allison and Pratt, 2006). Persistent increases in GluR1 subunit levels occur in the amygdala, nucleus accumbens and the VTA following repeated cocaine administration (Fitzgerald et al., 1996; Lu et al., 2003), and mice deficient in the GluR1 subunit show blunted morphine withdrawal (Vekovischeva et al., 2001). Using an immunohistochemical approach, Izzo et al (2001) showed upregulation of GluR1-subunit protein in dendritic regions of hippocampal pyramidal cells in rats withdrawn from diazepam, also coincident with the appearance of withdrawal anxiety. In many of these paradigms, including withdrawal from 1-week FZP exposure, AMPAR antagonists ameliorate both the alterations in GluR1 subunit expression and drug withdrawal behaviors including anxiety (Nestler, 2002; Van Sickle et al., 2004; Xiang et al., 2007). Collectively, these data suggest that increased synaptic incorporation of GluR1 containing-AMPARs is important for the acquisition or expression of drug withdrawal behaviors that occurs upon discontinuation of a variety of drugs of abuse. To our knowledge, the present electron microscopic study is the first to demonstrate enhanced incorporation of GluR1-containing receptors into excitatory synapses in the hippocampus during benzodiazepine withdrawal using a post-embedding immunogold approach. This study and previous reports suggest the possibility that blockade of AMPAR mediated excitatory transmission may be a viable approach for prevention and reduction of signs of benzodiazepine dependence (Steppuhn and Turski, 1993) and development of novel anti-anxiety treatments (Xiang et al., 2007).

In conclusion, the electron microscopic findings reported here provide a mechanistic insight into the enhanced AMPAR glutamatergic transmission associated with drug withdrawal-anxiety. It will be important to determine how specific AMPAR subpopulations in hippocampal CA1 neurons are regulated during FZP withdrawal, and the relative contribution of GluR1 homomers and GluR1/2 and GluR2/3 heteromers to the increased glutamatergic strength in this brain region. The findings also underscore the notion that the adaptive strategies characteristic of drug withdrawal are similar to activity-dependent plasticity and highly conserved in the CNS.

Acknowledgments

The authors would like to thank Margerete Otting, Krista Pettee and Maria Berrocal for technical assistance. We gratefully acknowledge Dr. Robert Wenthold for providing a rabbit polyclonal anti-GluR1 antibody and Drs. Ronald Petralia and Ya-Xian Wang for the GluR2 KO and WT tissue.

Support/Grant Information: This work was supported by NIDA RO1-DA04075 and RO1-DA18342 and MCO Drug Abuse Research Program (E.I.T.) and NIDA pre-doctoral fellowship F30-DA041412 (S.M.L.)

Abbreviations

a.a	amino acids
AMPA	alpha-Amino-3-hydroxy-5-methylisoxazole-4-propionic acid
CNS	central nervous system
GABA	gamma-amino butyric acid type A

CON	control
FZP	flurazepam
LTP	long-term potentiation
mEPSCs	miniature excitatory postsynaptic currents
GluR	glutamate receptor
KO	knockout
SO	stratum oriens
SP	stratum pyramidale
SR	stratum radiatum
PSD	postsynaptic density
VTA	ventral tegmental area
WT	wild-type

References

Allison C, Pratt JA. Differential effects of two chronic diazepam treatment regimes on withdrawal anxiety and AMPA receptor characteristics. Neuropsychopharmacology. 2006; 3:602–619. [PubMed: 15970947]

Adesnik H, Nicoll RA. Conservation of glutamate receptor 2-containing AMPA receptors during long-term potentiation. J Neurosci. 2007; 27:4598–4602. [PubMed: 17460072]

Ashton D, Willems R, De Prins E, Wauquier A. Selective inhibition of synaptic versus non-synaptic epileptogenesis by NMDA antagonists in the in vitro hippocampus. Epilepsia. 1988; 29:321–329. [PubMed: 3371286]

Bateson AN. Basic pharmacologic mechanisms involved in benzodiazepine tolerance and withdrawal. Curr Pharm Des. 2002; 8:5–21. [PubMed: 11812247]

Boudreau AC, Reimers JM, Milovanovic M, Wolf ME. Cell surface AMPA receptors in the rat nucleus accumbens increase during cocaine withdrawal but internalize after cocaine challenge in association with altered activation of mitogen-activated protein kinases. J Neurosci. 2007; 27:10621–10635. [PubMed: 17898233]

Brown TC, Correia SS, Petrok CN, Esteban JA. Functional compartmentalization of endosomal trafficking for the synaptic delivery of AMPA receptors during long-term potentiation. J Neurosci. 2007; 27:13311–13315. [PubMed: 18045925]

Carlezon WA Jr, Boundy VA, Haile CN, Lane SB, Kalb RG, Neve RL, Nestler EJ. Sensitization to morphine induced by viral-mediated gene transfer. Science. 1997; 277:812–814. [PubMed: 9242609]

Chang PY, Taylor PE, Jackson MB. Voltage imaging reveals the CA1 region at the CA2 border as a focus for epileptiform discharges and long-term potentiation in hippocampal slices. J Neurophysiol. 2007; 98:1309–1322. [PubMed: 17615129]

Chouinard G. Issues in the clinical use of benzodiazepines: potency, withdrawal, and rebound. J Clin Psychiatry. 2004; 65:7–12. [PubMed: 15078112]

Elias GM, Nicoll RA. Synaptic trafficking of glutamate receptors by MAGUK scaffolding proteins. Trends Cell Biol. 2007; 7:343–352. [PubMed: 17644382]

Engin E, Treit D. The role of hippocampus in anxiety: intracerebral infusion studies. Behav Pharmacol. 2007; 18:365–374. [PubMed: 17762507]

Fitzgerald LW, Ortiz J, Hamedani AG, Nestler EJ. Drugs of abuse and stress increase the expression of GluR1 and NMDAR1 glutamate receptor subunits in the rat ventral tegmental area: common adaptations among cross-sensitizing agents. J Neurosci. 1996; 16:274–282. [PubMed: 8613793]

Griffiths RR, Johnson MW. Relative abuse liability of hypnotic drugs: a conceptual framework and algorithm for differentiating among compounds. J Clin Psychiatry. 2005; 66:31–41. [PubMed: 16336040]

Greger IH, Esteban JA. AMPA receptor biogenesis and trafficking. Curr Opin Neurobiol. 2007; 3:289–297. [PubMed: 17475474]

Harris KM, Fiala JC, Ostroff L. Structural changes at dendritic spine synapses during long-term potentiation. Philos Trans R Soc Lond B Biol Sci. 2003; 358:745–748. [PubMed: 12740121]

Hayashi Y, Shi SH, Esteban JA, Piccini A, Poncer JC, Malinow R. Driving AMPA receptors into synapses by LTP and CaMKII: requirement for GluR1 and PDZ domain interaction. Science. 2000; 287:2262–2267. [PubMed: 10731148]

Hainfeld JFA. Small gold-conjugated antibody label: Improved resolution for electron microscopy. Science. 1987; 236:450–453. [PubMed: 3563522]

Hermann R, Walther P, Müller M. Immunogold labeling in scanning electron microscopy. Histochem Cell Biol. 1996; 106:31–39. [PubMed: 8858365]

Izzo E, Auta J, Impagnatiello F, Pesold C, Guidotti A, Costa E. Glutamic acid decarboxylase and glutamate receptor changes during tolerance and dependence to benzodiazepines. Proc Natl Acad Sci USA. 2001; 98:3483–3488. [PubMed: 11248104]

Joshi I, Shokralla S, Titis P, Wang LY. The role of AMPA receptor gating in the development of high-fidelity neurotransmission at the calyx of Held synapse. J Neurosci. 2004; 24:183–196. [PubMed: 14715951]

Jensen V, Kaiser KM, Borchardt T, Adelmann G, Rozov A, Burnashev N, Brix C, Frotscher M, Andersen P, Hvalby Ø, Sakmann B, Seeburg PH, Sprengel R. A juvenile form of postsynaptic hippocampal long-term potentiation in mice deficient for the AMPA receptor subunit GluR-A. J Physiol. 2003; 553:843–856. [PubMed: 14555717]

Jia Z, Agopyan N, Miu P, Xiong Z, Henderson J, Gerlai R, Taverna FA, Velumian A, MacDonald J, Carlen P, Abramow-Newerly W, Roder J. Enhanced LTP in mice deficient in the AMPA receptor GluR2. Neuron. 1996; 17:945–956. [PubMed: 8938126]

Jonas P, Burnashev N. Molecular mechanisms controlling calcium entry through AMPA-type glutamate receptor channels. Neuron. 1995; 15:987–990. [PubMed: 7576666]

Kauer JA, Malenka RC. Synaptic plasticity and addiction. Nat Rev Neurosci. 2007; 11:844–858. [PubMed: 17948030]

Khazaria VN, Weinberg RJ. Immunogold localization of AMPA and NMDA receptors in somatic sensory cortex of albino rat. J Comp Neurol. 1999; 412:292–302. [PubMed: 10441757]

Kim TJ, Ye EA, Jeon CJ. Distribution of AMPA glutamate receptor GluR1 subunit-immunoreactive neurons and their co-localization with calcium-binding proteins and GABA in the mouse visual cortex. Mol Cells. 2006; 21:34–41. [PubMed: 16511345]

King AE, Chung RS, Vickers JC, Dickson TC. Localization of glutamate receptors in developing cortical neurons in culture and relationship to susceptibility to excitotoxicity. J Comp Neurol. 2006; 498:277–294. [PubMed: 16856139]

Lang C, Barco A, Zablow L, Kandel ER, Siegelbaum SA, Zakharenko SS. Transient expansion of synaptically connected dendritic spines upon induction of hippocampal long-term potentiation. Proc Natl Acad Sci USA. 2004; 101:16665–16670. [PubMed: 15542587]

Lee HK, Takamiya K, Han JS, Man H, Kim CH, Rumbaugh G, Yu S, Ding L, He C, Petralia RS, Wenthold RJ, Gallagher M, Huganir RL. Phosphorylation of the AMPA receptor GluR1 subunit is required for synaptic plasticity and retention of spatial memory. Cell. 2003; 112:631–643. [PubMed: 12628184]

Lu L, Grimm JW, Shaham Y, Hope BT. Molecular neuroadaptations in the accumbens and ventral tegmental area during the first 90 days of forced abstinence from cocaine self-administration in rats. J Neurochem. 2003; 85:1604–1613. [PubMed: 12787079]

Malenka RC, Bear MF. LTP and LTD: an embarrassment of riches. Neuron. 2004; 44:5–21. [PubMed: 15450156]

Malinow R, Malenka RC. AMPA receptor trafficking and synaptic plasticity. Annu Rev Neurosci. 2002; 25:103–126. [PubMed: 12052905]

Matsubara A, Laake JH, Davanger S, Usami S, Ottersen OP. Organization of AMPA receptor subunits at a glutamate synapse: a quantitative immunogold analysis of hair cell synapses in the rat organ of Corti. J Neurosci. 1996; 16:4457–4467. [PubMed: 8699256]

McNaughton N, Gray JA. Anxiolytic action on the behavioural inhibition system implies multiple types of arousal contribute to anxiety. J Affect Disord. 2000; 61:161–176. [PubMed: 11163419]

Molleman A, Little HJ. Increases in non-N-methyl-D-aspartate glutamatergic transmission, but no change in gamma-aminobutyric acid B transmission, in CA1 neurons during withdrawal from in vivo chronic ethanol treatment. J Pharmacol Exp Ther. 1995; 274:1035–1041. [PubMed: 7562466]

Megias M, Emri Z, Freund TF, Gulyas AI. Total number and distribution of inhibitory and excitatory synapses on hippocampal CA1 pyramidal cells. Neuroscience. 2001; 102:527–540. [PubMed: 11226691]

Nestler EJ. Common molecular and cellular substrates of addiction and memory. Neurobiol Learn Mem. 2002; 78:637–647. [PubMed: 12559841]

Nicoll RA. Expression mechanisms underlying long-term potentiation: a postsynaptic view. Philos Trans R Soc Lond B Biol Sci. 2003; 358:721–726. [PubMed: 12740118]

Nusser Z, Lujan R, Laube G, Roberts JD, Molnar E, Somogyi P. Cell type and pathway dependence of synaptic AMPA receptor number and variability in the hippocampus. Neuron. 1998; 21:545–559. [PubMed: 9768841]

Oh MC, Derkach VA. Dominant role of the GluR2 subunit in regulation of AMPA receptors by CaMKII. Nat Neurosci. 2005; 8:853–854. [PubMed: 15924137]

Petralia RS, Wenthold RJ. Light and electron immunocytochemical localization of AMPA-selective glutamate receptors in the rat brain. J Comp Neurol. 1992; 318:329–354. [PubMed: 1374769]

Petralia RS, Wang YX, Mayat E, Wenthold RJ. Glutamate receptor subunit 2-selective antibody shows a differential distribution of calcium-impermeable AMPA receptors among populations of neurons. J Comp Neurol. 1997; 385:456–476. [PubMed: 9300771]

Petralia RS, Esteban JA, Wang YX, Partridge JG, Zhao HM, Wenthold RJ, Malinow R. Selective acquisition of AMPA receptors over postnatal development suggests a molecular basis for silent synapses. Nat Neurosci. 1999; 2:31–36. [PubMed: 10195177]

Poncer JC. Hippocampal long term potentiation: silent synapses and beyond. J Physiol. 2003; 97:415–422.

Plant K, Pelkey KA, Bortolotto ZA, Morita D, Terashima A, McBain CJ, Collingridge GL, Isaac JT. Transient incorporation of native GluR2-lacking AMPA receptors during hippocampal long-term potentiation. Nat Neurosci. 2006; 5:602–604. [PubMed: 16582904]

Sanchis-Segura C, Borchardt T, Vengeliene V, Zghoul T, Bachteler D, Gass P, Sprengel R, Spanagel R. Involvement of the AMPA receptor GluR-C subunit in alcohol-seeking behavior and relapse. J Neurosci. 2006; 26:1231–1238. [PubMed: 16436610]

Sans N, Vissel B, Petralia RS, Wang YX, Chang K, Royle GA, Wang CY, O'Gorman S, Heinemann SF, Wenthold RJ. Aberrant formation of glutamate receptor complexes in hippocampal neurons of mice lacking the GluR2 AMPA receptor subunit. J Neurosci. 2003; 23:9367–73. [PubMed: 14561864]

Sassoe-Pognetto M, Ottersen OP. Organization of ionotropic glutamate receptors at dendrodendritic synapses in the rat olfactory bulb. J Neurosci. 2000; 20:2192–2201. [PubMed: 10704494]

Shi S, Hayashi Y, Esteban JA, Malinow R. Subunit-specific rules governing AMPA receptor trafficking to synapses in hippocampal pyramidal neurons. Cell. 2001; 105:331–343. [PubMed: 11348590]

Song J, Shen G, Greenfield LJ Jr, Tietz EI. Benzodiazepine withdrawal-induced glutamatergic plasticity involves up-regulation of GluR1-containing alpha-amino-3-hydroxy-5-methylisoxazole-4-propionic acid receptors in hippocampal CA1 neurons. J Pharmacol Exp Ther. 2007; 322:569–581. [PubMed: 17510319]

Steppuhn KG, Turski L. Diazepam dependence prevented by glutamate antagonists. Proc Natl Acad Sci USA. 1993; 90:6889–6893. [PubMed: 8341715]

Takumi Y, Ramirez-Leon V, Lakke P, Rinvik E, Ottersen OP. Different modes of expression of AMPA and NMDA receptors in hippocampal synapses. Nature Neurosci. 1999; 2:618–624. [PubMed: 10409387]

Tietz EI, Zeng XJ, Chen S, Lilly SM, Rosenberg HC, Kometiani P. Antagonist-induced reversal of functional and structural measures of hippocampal benzodiazepine tolerance. J Pharmacol Exp Ther. 1999; 291:932–942. [PubMed: 10565808]

Valtschanoff JG, Burette A, Davare MA, Leonard AS, Hell JW, Weinberg RJ. SAP97 concentrates at the postsynaptic density in cerebral cortex. Eur J Neurosci. 2000; 12:3605–3614. [PubMed: 11029631]

Van Sickle BJ, Tietz EI. Selective enhancement of AMPA receptor-mediated function in hippocampal CA1 neurons from chronic benzodiazepine-treated rats. Neuropharmacology. 2002; 43:11–27. [PubMed: 12213255]

Van Sickle BJ, Xiang K, Tietz EI. Transient plasticity of hippocampal CA1 neuron glutamate receptors contributes to benzodiazepine withdrawal-anxiety. Neuropsychopharmacology. 2004; 29:1994–2006. [PubMed: 15266351]

Vekovischeva OY, Zamanillo D, Echenko O, Seppala T, Uusi-Oukari M, Honkanen A, Seeburg PH, Sprengel R, Korpi ER. Morphine-induced dependence and sensitization are altered in mice deficient in AMPA-type glutamate receptor-A subunits. J Neurosci. 2001; 21:4451–4459. [PubMed: 11404432]

Wafford KA. $GABA_A$ receptor subtypes: any clues to the mechanism of benzodiazepine dependence? Curr Opin Pharmacol. 2005; 5:47–52. [PubMed: 15661625]

Washburn MS, Numberger M, Zhang S, Dingledine R. Differential dependence on GluR2 expression of three characteristic features of AMPA receptors. J Neurosci. 1997; 17:9393–9406. [PubMed: 9390995]

Wenthold RJ, Yokotani N, Doi K, Wada K. Immunochemical characterization of the non-NMDA glutamate receptor using subunit-specific antibodies. Evidence for a hetero-oligomeric structure in rat brain. J Biol Chem. 1992; 267:501–507. [PubMed: 1309749]

Wenthold RJ, Petralia RS, Blahos J, Niedzielski AS. Evidence for multiple AMPA receptor complexes in hippocampal CA1/CA2 neurons. J Neurosci. 1996; 16:1982–1989. [PubMed: 8604042]

Whitlock JR, Heynen AJ, Shuler MG, Bear MF. Learning induces long-term potentiation in the hippocampus. Science. 2006; 313:1093–1097. [PubMed: 16931756]

Xiang K, Tietz EI. Benzodiazepine-induced hippocampal CA1 neuron alpha-amino-3-hydroxy-5-methylisoxasole-4-propionic acid (AMPA) receptor plasticity linked to severity of withdrawal anxiety: differential role of voltage-gated calcium channels and N-methyl-D-aspartic acid receptors. Behav Pharmacol. 2007; 18:447–460. [PubMed: 17762513]

Xie XH, Tietz EI. Reduction in potency of selective gamma-aminobutyric acid A agonists and diazepam in CA1 region of in vitro hippocampal slices from chronic flurazepam-treated rats. J Pharmacol Exp Ther. 1992; 262:204–211. [PubMed: 1320683]

Zamanillo D, Sprengel R, Hvalby O, Jensen V, Burnashev N, Rozov A, Kaiser KM, Koster HJ, Borchardt T, Worley P, Lubke J, Frotscher M, Kelly PH, Sommer B, Andersen P, Seeburg PH, Sakmann B. Importance of AMPA receptors for hippocampal synaptic plasticity but not for spatial learning. Science. 1999; 284:1805–1811. [PubMed: 10364547]

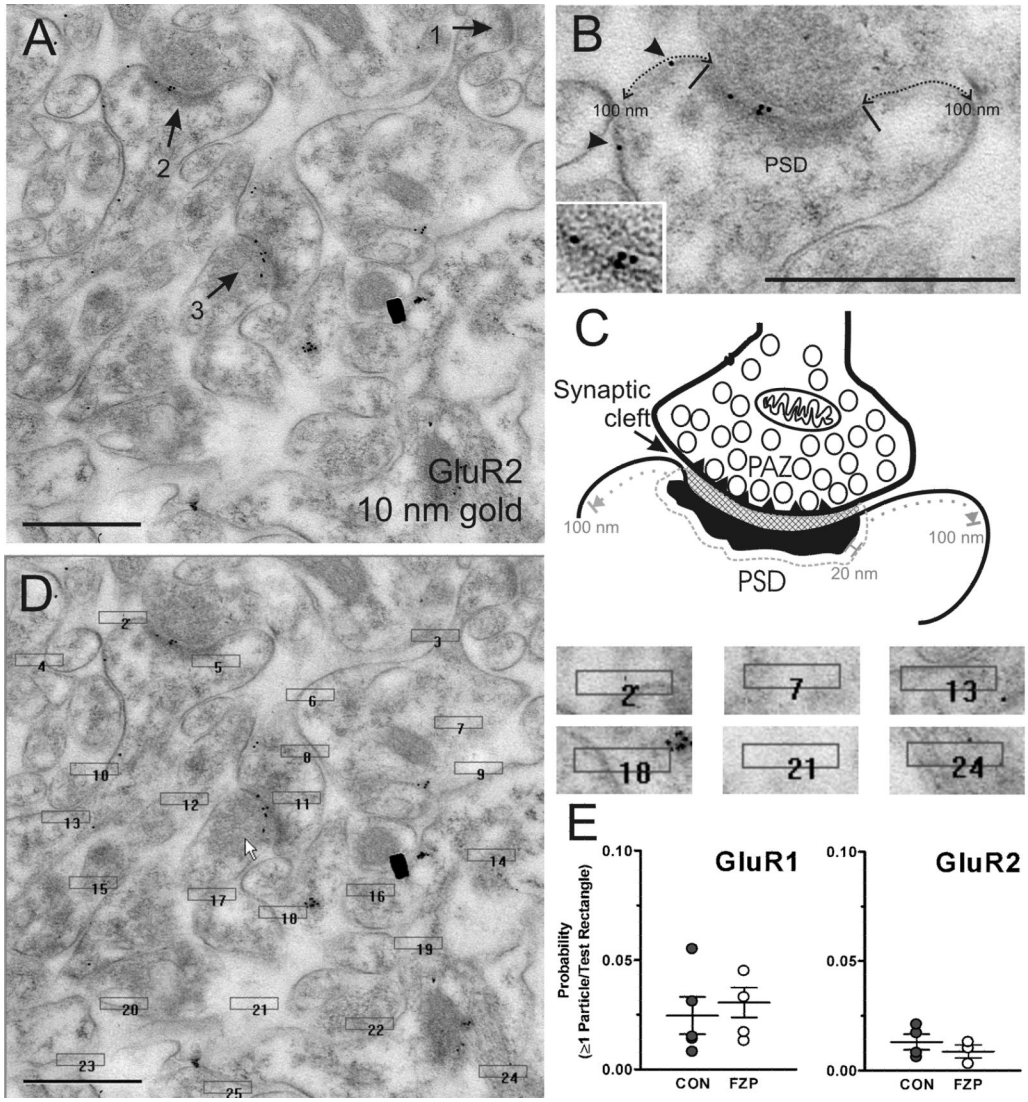

Figure 1.

Location of immunogold labeling. **(A)** Full-field image of a digital electron micrograph of the CA1 SR region used in the analysis and containing three synapses (arrows 1, 2 and 3). Two of them contain GluR2-immunogold labeling (10 nm particles). All the synapses analyzed are clearly asymmetric and many can be identified on spine heads. **(B)** Magnified view of synapse 2 showing the lateral edges of the PSD region (black bars), extrasynaptic GluR2-immunolabeling (arrowheads) and the approximate 100 nm plasma membrane regions that were considered as "perisynaptic" on these cross-section analyses (dotted line). The inset shows labeling at high contrast to better define pre-and postsynaptic membranes. **(C)** Depicts a diagram of a synapse similar to the one shown in **B** marking the presynaptic active zone (PAZ) (triangles inserted in the membrane of the presynaptic bouton), opposed by a synaptic cleft (generally more electron-dense than the extrasynaptic intercellular space) and the PSD region. Immunogold particles related to the PSD were counted if they were located within a 20 nm boundary region surrounding the edges of the PSD. This region included all the synaptic cleft area. Particles were considered extrasynaptic if clearly located on the membrane and within a 100 nm distance of the PSD (excluding the 20 nm drop zone associated with the PSD). **(D)** Test rectangles on top of the image shown in **A**. The

immunogold content in these rectangles was used to calculate the probability that one or more particles were randomly associated with a region similar to the PSD. Test rectangles were 0.22 × 0.045 μm in size and randomly placed on the images. **(E)** The probabilities that one or more gold particle was related to a test rectangle was less than 5% in both GluR1 and GluR2 labeled synapses in both control and FZP-withdrawn rats. Scale bars in A, B and D are 0.5 μm.

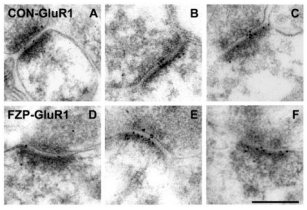

Figure 2.

Electron micrographs of AMPAR GluR1 subunit immunogold labeling in hippocampal CA1 SR from control and FZP-withdrawn rats. **(A-C)** Representative images of GluR1-labeled (Chemicon) asymmetric synapses from control rats. Immunogold particles (10 nm) are located primarily within the postsynaptic density (PSD) and extend into the synaptic cleft. (**D-F)** Representative images of GluR1-labeled asymmetric synapses from FZP-withdrawn rats also show immunogold labeling within the PSD and synaptic cleft. GluR1 immunogold labeling was significantly increased in FZP-withdrawn CA1 synapses compared to controls (see Table 1 and Fig. 3). Scale bar in F is 0.25 μm. All images are at the same magnification.

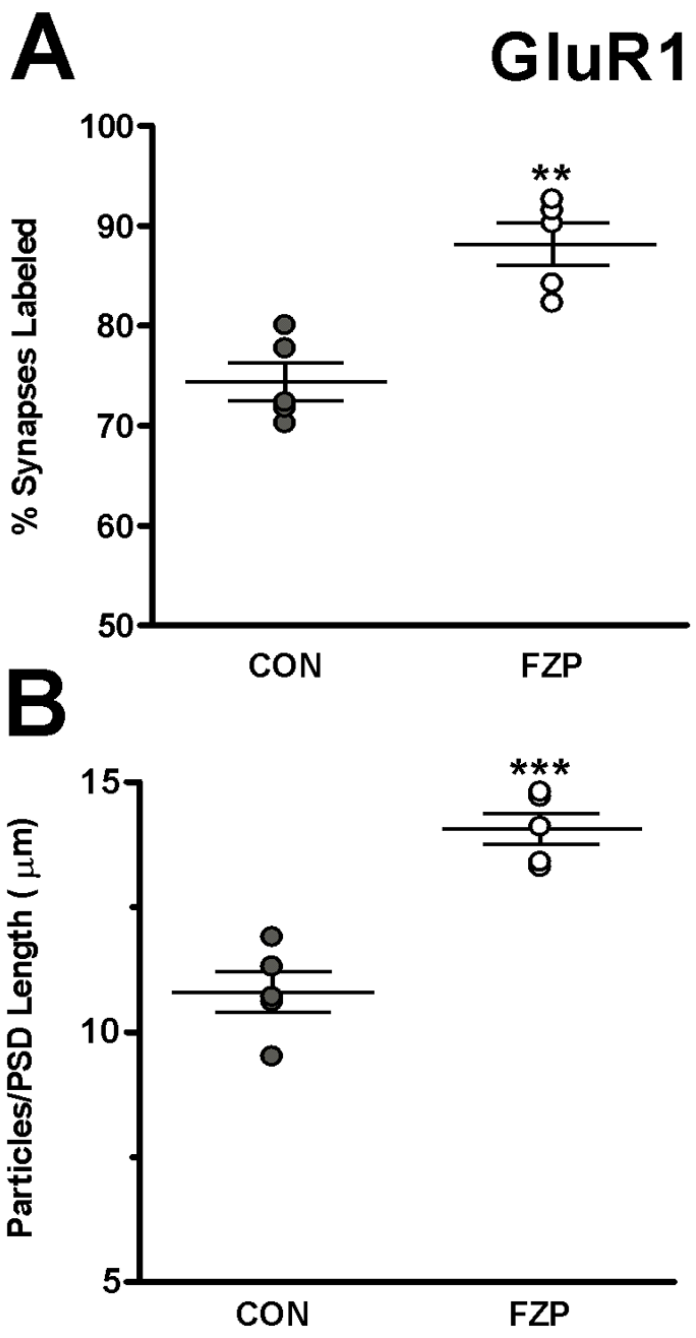

Figure 3.

FZP-withdrawal increases AMPAR GluR1 subunit incorporation in hippocampal CA1 asymmetric synapses. **(A)** The percentage of synapses with immunogold labeling for GluR1 was significantly higher (**p<0.01) in synapses from FZP-withdrawn rats compared to controls. **(B)** GluR1 immunogold density estimated by the number of gold particles per micron length of synapse was also significantly increased in synapses from FZP-withdrawn rats compared to controls (n=5 rats/group, ***p<0.001). Error bars indicate S.E.M.'s.

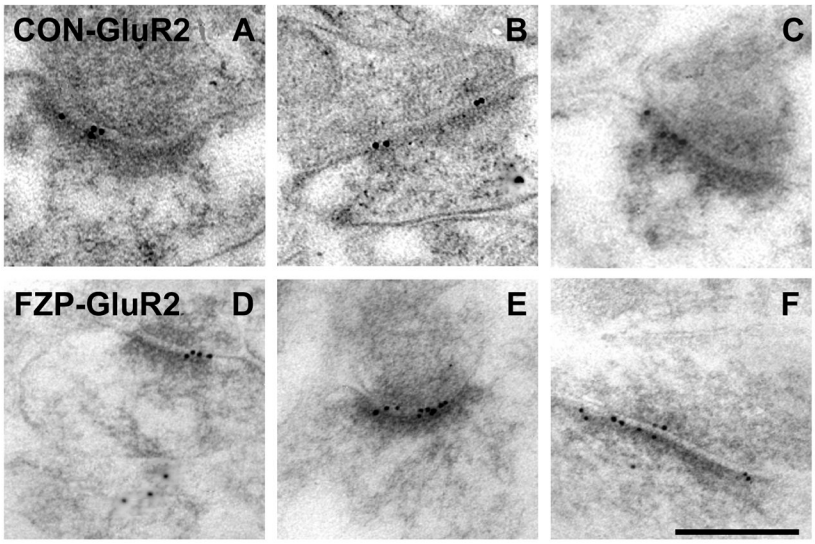

Figure 4.

Electron micrographs of AMPAR GluR2 subunit immunogold labeling in hippocampal CA1 SR from control and FZP-withdrawn rats. **(A-C)** Representative images of GluR2-labeled (Chemicon) asymmetric synapses from control rats show immunogold particles (10 nm) mainly in the postsynaptic density and extending into the synaptic cleft. **(D-F)** GluR2 immunogold labeling was unchanged between control and FZP-withdrawn CA1 neuron synapses (see Table 1 and Fig. 5). Scale bar in F is 0.25 μm. All images are at the same magnification.

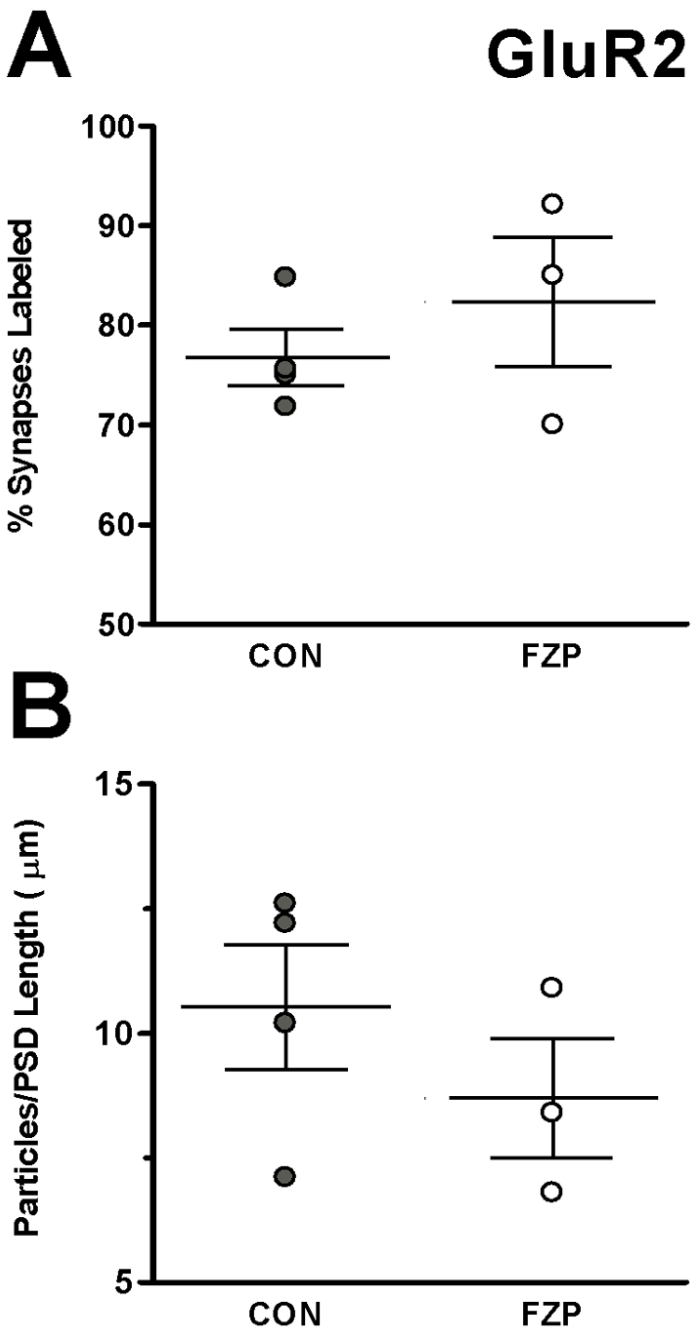

Figure 5.

FZP-withdrawal has no effect on AMPAR GluR2 subunit incorporation in hippocampal CA1 asymmetric synapses. In contrast to changes observed in GluR1 immunogold labeling during FZP-withdrawal, no significant (p>0.05) changes in either percentage of synapses labeled **(A)** or mean GluR2 immunogold density **(B)** was observed between the two groups (n=4 control and 3 FZP-withdrawn rats/group). Error bars indicate S.E.M.'s.

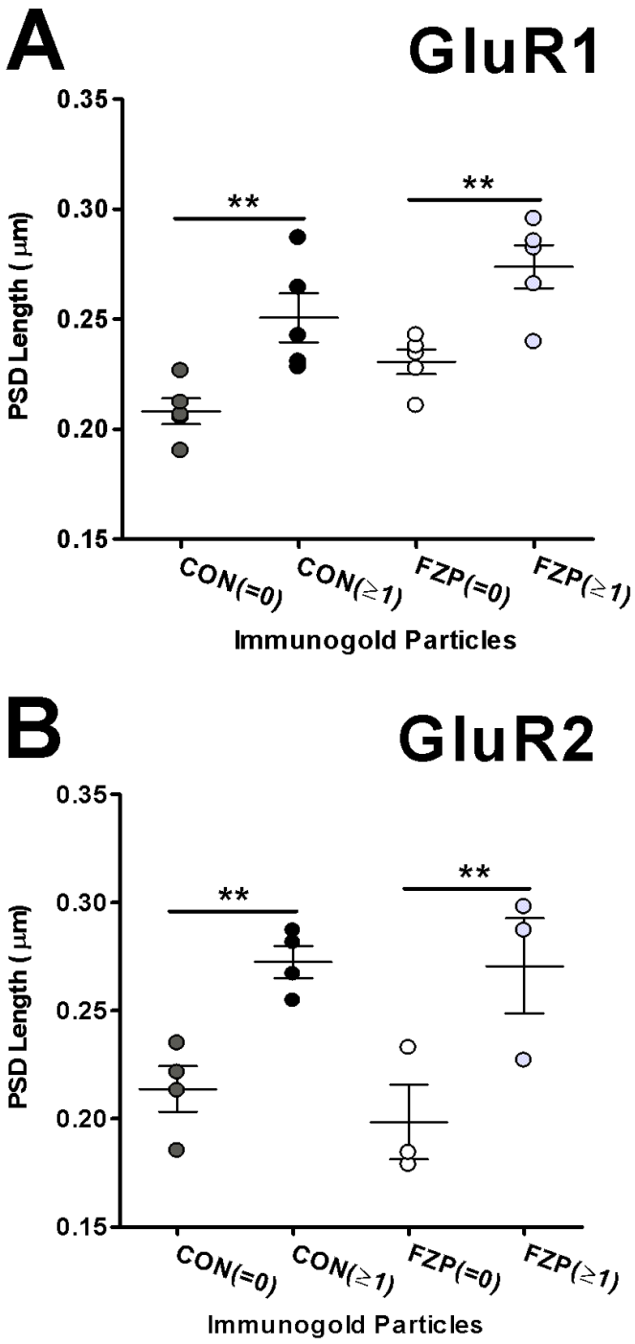

Figure 6.

Analysis of AMPA-immunonegative and immunopositive synapse size. **(A)** Analysis of PSD lengths in GluR1-labeled sections show that AMPAR immunonegative synapses (=0) are smaller than immunopositive synapses (≥1) in both control and FZP-withdrawn tissues (n=5 rats/group). **(B)** PSD lengths of immunonegative synapses from sections reacted with the GluR2 antibody were also significantly smaller than immunopositive synapses (**p<0.01).

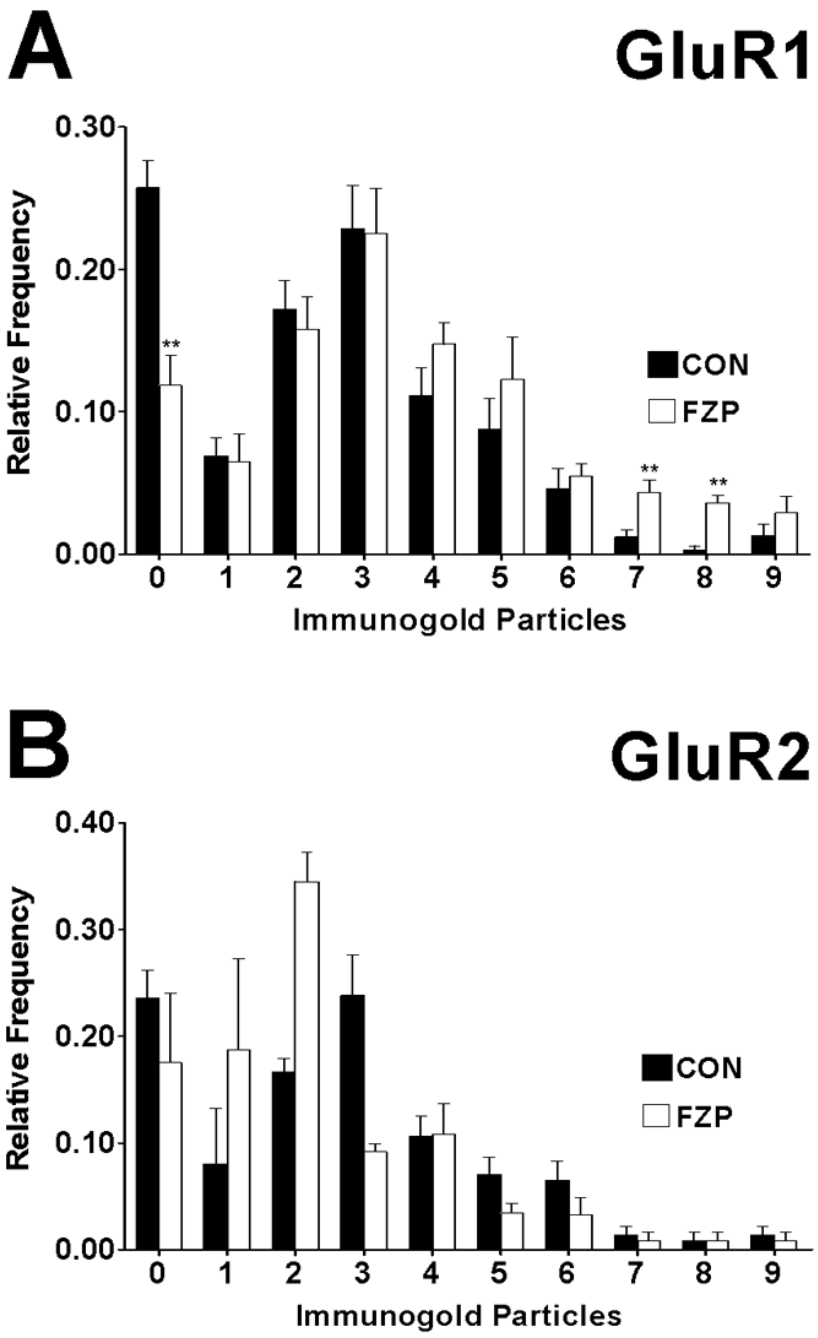

Figure 7.

Distribution histograms of synapses containing different numbers of GluR1 or GluR2 immunogold particles. **(A)** Histogram bars represent average relative frequencies of synapses without GluR1 gold particles (0 particles) or containing from 1 to 9 gold particles in control and FZP-withdrawn animals. The distributions of GluR1 particles in synapses from control (black bars) and FZP-withdrawn rats (open bars) were compared by χ^2 analysis and a significant overall increase in the number of synapses with a higher content of gold particles was detected in FZP-withdrawn rats compared to controls (χ^2=59.4, df=9, p=0.000). The fraction of synapses lacking GluR1 immunogold labeling was significantly lower in asymmetric synapses from FZP-withdrawn rats compared to control rats (**p<0.01,

Mann-Whitney U test). A significant increase in the fraction of synapses expressing 7 and 8 gold particles was also observed after FZP withdrawal (**p<0.01, Mann-Whitney U test). **(B)** The distributions of GluR2 immunogold particle content also significantly different in CA1 synapses from between control and FZP-withdrawn animals (χ^2=77.8, df=9, ***p=0.000). However, the observed fraction of synapses lacking GluR2 particles (0 particles) was not significantly different between groups (p=0.86, Mann-Whitney U test), nor were there differences in any fraction of labeled synapses with a given number of gold particles (1 to ≥9; p>0.05, Mann-Whitney U test).

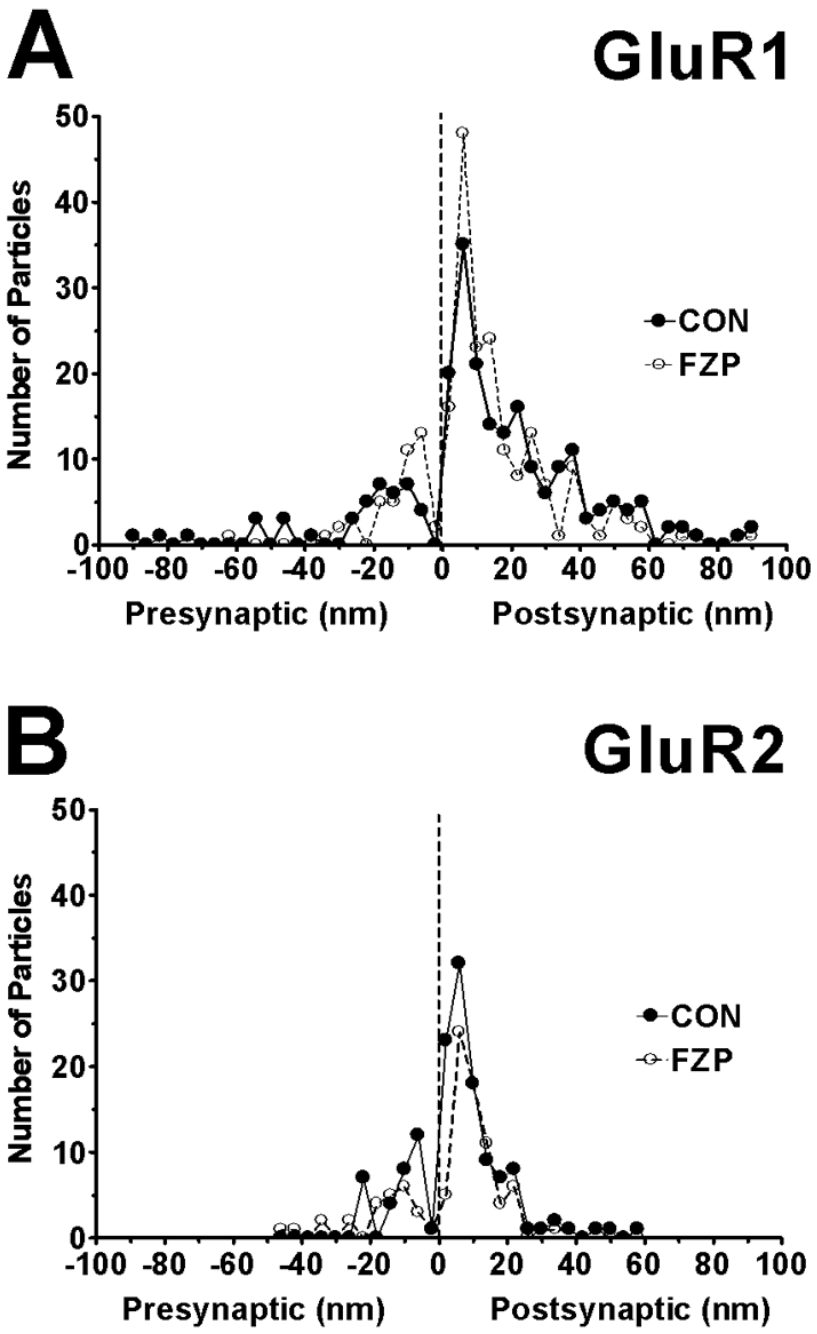

Figure 8.

Spatial distribution of all **(A)** GluR1, **(B)** GluR2 immunogold particles found within 100 nm of the postsynaptic membrane on either the extracellular or cytoplasmic side. Asymmetric synapses with clearly visible and well-defined PSDs and synaptic clefts were digitally imaged at a final magnification of X 36,000. The distances between centers of each 10 nm gold particle to the outer leaflet of postsynaptic membrane were measured and grouped into 4 nm wide bins (0 on the abscissa represents external face of postsynaptic membrane). Negative values indicate gold particles located at a distance from the postsynaptic membrane and in the direction of the presynaptic bouton and synaptic cleft (average width ~20 nm). Positive values indicate immunogold labeling on the cytoplasmic side. GluR1 and

GluR2-immunogold labeling for both subunit antibodies peaked 6 nm inside the postsynaptic membrane (resolution ±2 nm) with GluR1 labeling extending more distally towards the cytoplasmic side than GluR2 labeling. The majority of both GluR1 and GluR2 immunolabeling was located within the PSD region (width ~45 nm). Very few immunogold particles were detected extracellularly, beyond the synaptic cleft (values <−20 nm). Thus, both the GluR1 and GluR2 immunolabeling analyzed was very tightly related to the extent of the PSD. Data was obtained from 67 (CON) and 56 (FZP) synapses in GluR1-labeled tissues and from 44 (CON) and 40 (FZP) synapses in GluR2-labeled tissues.

Table 1

GluR1 Subunit Immunogold Labeling

Rat #	Synapses Sampled	Labeled (%)≥1 Particle	Particles/PSD Length (μm)	PSD Length (μm)	PSD Thickness (μm)	PSD Area (μm)^2
Control						
1	67	70.2	10.6	0.231	0.061	0.014
2	46	71.7	10.7	0.228	0.070	0.017
3	54	77.7	11.3	0.222	0.058	0.013
4	50	80.0	11.9	0.272	0.047	0.012
5	46	71.7	9.5	0.242	0.058	0.015
Mean ±SEM	= 263	**74.4 ±1.9**	**10.8 ±0.4**	**0.239 ±0.009**	**0.059 ±0.004**	**0.014 ±0.001**
FZP-Withdrawn						
1	56	82.2	14.1	0.286	0.056	0.016
2	57	84.2	13.3	0.241	0.064	0.015
3	54	92.6	14.7	0.278	0.062	0.018
4	59	91.5	14.8	0.263	0.059	0.016
5	51	90.2	13.4	0.281	0.067	0.019
Mean ±SEM	= 277	**88.2 ±2.2****	**14.1 ±0.3*****	**0.270 ±0.008***	**0.062 ±0.002**	**0.017 ±0.001**
***p* Value**		**0.008**	**0.0002**	**0.01**	**0.52**	**0.051**

Table 2

GluR2 Subunit Immunogold Labeling

Rat #	Synapses Sampled	Labeled (%)±1 Particle	Particles/PSD Length (μm)	PSD Length (μm)	PSD Thickness (μm)	PSD Area (μm)^2
Control						
1	44	75.0	12.2	0.253	0.056	0.013
2	44	75.0	10.2	0.246	0.050	0.013
3	33	84.8	12.6	0.282	0.058	0.017
4	39	71.8	7.1	0.254	0.062	0.016
Mean ±SEM	=160	**76.7 ±2.8**	**10.5 ±1.3**	**0.259 ±0.008**	**0.057 ±0.003**	**0.015 ±0.001**
FZP-Withdrawn						
1	40	70.0	8.4	0.278	0.092	0.024
2	41	85.0	10.9	0.221	0.043	0.010
3	38	92.1	6.8	0.279	0.056	0.017
Mean ±SEM	=119	**82.3 ±6.5**	**8.7 ±1.2**	**0.259 ±0.019**	**0.064 ±0.015**	**0.017 ±0.004**
***p* Value**		0.70	0.35	0.98	0.59	0.62